Flip-and-Leap in a Hexapod Robot

Shou-Li Hsu, Kuan-Wei Liu, Chia-Ho Hsiung, Syuan-Yu Chen, Ting-Hao Wang, and Pei-Chun Lin

***Abstract*—This article introduces the behavior development of a flip-and-leap gait in an RHex-style hexapod robot. Owing to the dynamic characteristics of the behavior, as well as the limited actuation freedom of the RHex-style robot, the development relies on understanding the dynamics of the robot through its reduced-order representation. The model consists of a planar rigid body and three spring-loaded compliant rolling legs. The parameters and initial motion conditions were varied to evaluate the dynamic response of the model, providing the control hint to initiate such behaviors. The proposed strategy was experimentally validated, and the results confirm that the RHex-style robot can perform a flip-and-leap behavior, which could be useful for negotiating harsh terrain.**

***Index Terms*—hexapod robot, model, flipping, leaping, gait**

I. Introduction

BIONICS [1-8], getting inspiration from nature to solve technological problems, has not been out of fashion in science research since it was proposed in the 1960s. The application of bionics is extremely broad. For instance, the design and construction of interior space in a hospital were inspired by the anti-microorganism skin of sharks, and the environmentally friendly structure without an air-conditioning system was inspired by a climate control behavior performed by termites.

The hexapod robot, or RHex [9], is a classic application of robotics in bionics, as shown in Fig. 1(a). Developed from observing and intimating the motion of cockroaches, though RHex only has one rotational degree-of-freedom per leg, it is good at negotiating challenging terrains. With powerful motors, a high-capacity battery, and diverse sensors, the robot can complete behaviors. It can also carry out advanced missions such as going up and down stairs, climbing over an obstacle, and self-righting as it falls over [10]. Some researchers have replaced the legs with other shapes or materials for special purposes. For example, AQUA could swim underwater with fins [11], and the Wheel-RHex moves smoothly and efficiently on a flat floor using changeable wheels. Moreover, there are robots developed for military use with waterproof, anti-dust aluminum cases, larger battery capacity and more powerful motors, such as Rugged RHex.

In addition to a variety of novel mechanism designs, the gait design enables the robots to have greater agility for negotiating the environment. Some dynamic behaviors have been conducted with RHex, such as running [12], stair ascent [13, 14], stair descent [15], bounding [16], pronking [17], self-righting [10], and leaping [18], by finding an appropriate state sequence. In this research, we focused on the flipping and leaping gait for the advantages of its outstanding ability to negotiate obstacles. For a hexapod robot, flipping provides great vertical displacement for the body centroid and allows the robot to perform more complicated actions. However, as terrain becomes rougher, leaping becomes more appropriate because it requires little ground contact to overcome the terrains. Therefore, the development and combination of a flipping and leaping gait improves the traversing ability of RHex.

This work is supported by Ministry of Science and Technology (MoST), Taiwan, under contract: MOST 107-2634-F-002-004-, MOST 108-2634-F-002-002-, and MOST 109-2634-F-002-039-.

Authors are in the department of Mechanical Engineering, National Taiwan University (NTU), No.1 Roosevelt Rd. Sec.4, Taipei 106, Taiwan. (Corresponding email: peichunlin@ntu.edu.tw).

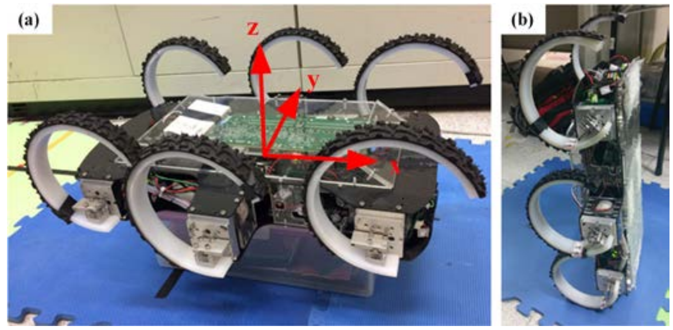

Figure 1. The RHex-style robot: (a) in resting posture and (b) in erect posture.

Based on our previous model-based strategy for initiating a robot's dynamic behavior, we aimed to understand the flipping/leaping mechanism. More specifically, a planar rigid-body model with three compliant C-shaped legs was constructed so that the force and moment, as well as the resultant motion to the body, could be investigated. The model had spring-loaded compliant legs with rolling contact, and the configuration was similar to the two-rolling-leg model as previously reported [19]. Compared with a previous study of running [12] and running-to-leaping maneuvers [18] in a hexapod robot, this study explored a wider parameter domain and focused on the key factors that determined the initiation of either leaping or flipping behaviors from a resting and running posture. The contributions of the study include 1) analysis of the parameters that affect the model's leaping or flipping behaviors; and 2) a model-based approach so that the empirical robot can perform the desired behavior without exhaustive searching or testing.

The remainder of this paper is organized as follows: Section II introduces the flipping gait algorithm; Section III describes the simulation settings and the consequences of the model with varying parameters; Section IV reports the experimental results using an RHex robot; and Section V concludes the work.

II. Flipping and Flipping-Related Gaits Algorithm

A. Introduction of Flipping and Flipping-Related Gaits

The flipping model was symmetric with respect to the x-axis along the long side of the body, as defined in Fig. 1(a), whereas the rotational axis was parallel to the y-axis. During the flipping process, the robot first lies down with the end of the legs touching the ground, as shown in Fig. 2(a). Next, the robot tilts the body with one end on the ground by giving the rear legs a torque command, as shown in Fig. 2(b). After a delay of several hundred milliseconds, the robot gives the middle and fore legs torque commands to increase the body pitch, denoted as θ_y, until flipping upside down, as shown in Fig. 2(c). After that, the six legs are set in the same phase, or what is called a standing posture, to prepare for landing, as shown in Fig. 2(d) and (e).

Continuous flipping combines the flipping and the reverse flipping, which uses the reverse of the execution sequence of each leg with opposite phase already mentioned, which enables the robot to flip back and forth to overcome obstacles such as a high step or a ditch. Alternatively, the flip-to-erect gait, as shown in Fig. 3, was used to stop the procedure while the body was maintained vertical by the fore legs, and it could be utilized to initiate further dynamic gaits.

B. The Flip-and-Leap Gait

The flipping gait, however, cannot make the robot move forward since the reacting forces from the ground are vertical, so the robot could only move up and down. Therefore, we further developed the flip-and-leap gait for the robot to leap forward and even leap up a step. The flip-and-leap gait is completed through a process of chained gaits, including tripod, flipping, and leaping. The detailed procedure, as shown in Fig. 4, could be separated into the following four steps:

1) RHex walks by tripod gait to the setting location where the robot is going to flip.
2) The robot makes a small leap, thrust by the set of all legs striking the ground (the first section of the leaping gait). The purpose of this small leap is to synchronize the phases of the six legs for the upcoming flip. Additionally, the increment of the body pitch during the small leap is also the key variable for the flipping afterward.
3) While the rear legs hit the ground, the robot executes the flipping gait by triggering the rear, middle, and fore legs chronologically. As the body lifts off the ground, the phases of the fore legs are set to the initial position for leaping.
4) Following the perception at the best pitch angle after the robot flips 90 degrees, the front legs step on the ground and push the robot forward and upward, which allows the robot up the step without leaning.

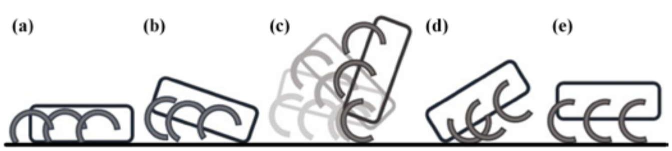

Figure 2. Flipping procedure initiated from (a) the resting posture; (b) and (c) the body was tilted through the sequence impulse driven by the rear legs, middle legs, and fore legs. Afterward, (d) the phases of the legs were synchronized to perform (e) the standing gait for landing.

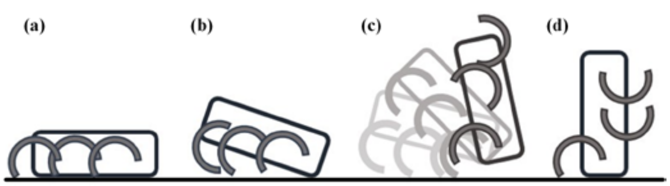

Figure 3. Flip-to-erect procedure initiated from (a) the resting posture. Next, (b) and (c) are the chronological impulses from the rear legs, mid legs, and fore legs that tilted the body. Finally, (d) the body was vertically maintained using the fore legs.

III. Simulation of the Flip-and-Leap Gait

A. Simulation Using the R-SLIP Model

To optimize the variables for triggering the complex flip-and-leap gait, we disassembled the complete flip-and-leap procedure into different sections and utilized the planar model with different initial conditions to evaluate the performance outcome. Among several template-style models, such as SLIP [20, 21], SLIP-T [22], and SLIP-R [23], we found that the successor of the R-SLIP [12], the TDR-SLIP [24] which configures a linear torsional spring and damper on an approximately half-circular, massless, and compliant rolling leg is resemble to the RHex leg, so it was adopted in the simulation. The simulation was implemented on MATLAB Simulink with separated subsystems, which simplified the process of deriving equations of motion under the complex combination of different gaits.

The planar model could move freely in the space and had a six degree-of-freedom (DOF) joint connected to the world frame, which provided geometric constraints and contact forces. We connected the solid body and legs of the robot to the sphere to plane force block introduced in the Contact Forces Library, and it was able to translate and rotate between the world frame

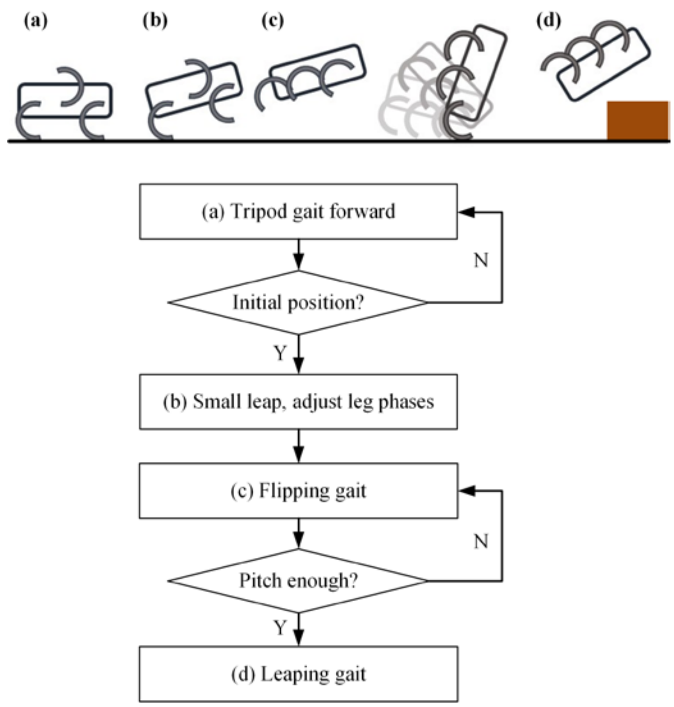

Figure 4. The sequential motion and a flow chart of the flip-and-leap behavior: (a) tripod walking/running, (b) small leaping, (c) flipping, and (d) leaping.

and the body frame. The knee joints were actuated by input torque profiles to implement the flipping and leaping gait, and the data, including the pitch angle θ_y, pitch angular velocity $\dot{\theta}_y$, and position and velocity of center of mass (CoM), were recorded for analysis. Here, we will focus on the leaping gait specifically since it is more complicated than others.

B. Analysis of the Flipping Gait

We explored the optimized body movement in the flipping gait with different parameters. The flipping gait involves three phases: the actuation of the rear legs, the middle legs, and the fore legs. The motion of each leg was commanded through torque control, and each motor performed maximum output with the same trajectory. The command latency for a separated set of legs, denoted as T_{rear}, T_{middle}, and T_{fore}, was the key for successful flipping. Without a proper delay time, the robot might leap height without flipping or could not overcome the gravitational force to flip upside down.

We started the analysis by assuming that T_{middle} and T_{fore} are independent and then plotted the variation of pitch angle θ_y under the different T_{middle} and T_{fore}, as shown in Fig. 5(a) and (b). We thus obtained a set of command latency with which the robot can achieve the maximum pitch angle θ_y.

To substantiate the assumption that T_{middle} and T_{fore} are independent, a trial simultaneously considered both variables, as shown in Fig. 6. The color plot represents the value of maximum pitch angle θ_y found among the time-sequence data. The variation trend of either T_{middle} or T_{fore} was roughly similar as the other parameter varied, and hence, we assumed the variables to be independent for simplification. Note that we did not always apply the best result from the simulation because the circumstances might require a specific initial condition during practical cases.

C. Analysis of Leaping Gait

In this section, we further discuss the dynamic effect of the leaping gait with different changes, including initial pitch angle, initial angle and stiffness of torsional springs on the leg, and the influences on the assistance of the fore and middle legs.

1) Initial Pitch Angle θ_{y,t_0}

Because the leaping gait came after the flipping gait, we assumed that the robot had fallen from the upright position. In consequence, it had a higher initial pitch angular velocity $\dot{\theta}_{y,t_0}$ with smaller initial pitch angle θ_{y,t_0}. When the θ_{y,t_0} went smaller, the friction was not enough to turn θ_y back because of the high $\dot{\theta}_y$, and the robot fell to the ground shortly after the start. In contrast, as the θ_{y,t_0} became larger, the duration of contact between the legs and the ground became longer and caused the robot to fall backward. Thus θ_{y,t_0} should be carefully selected so that the robot can leap as high as possible. Fig. 7(a) shows the CoM_g and θ_y with different θ_{y,t_0}. Thus, the proper θ_{y,t_0} was chosen to be about 40 to 45 degrees.

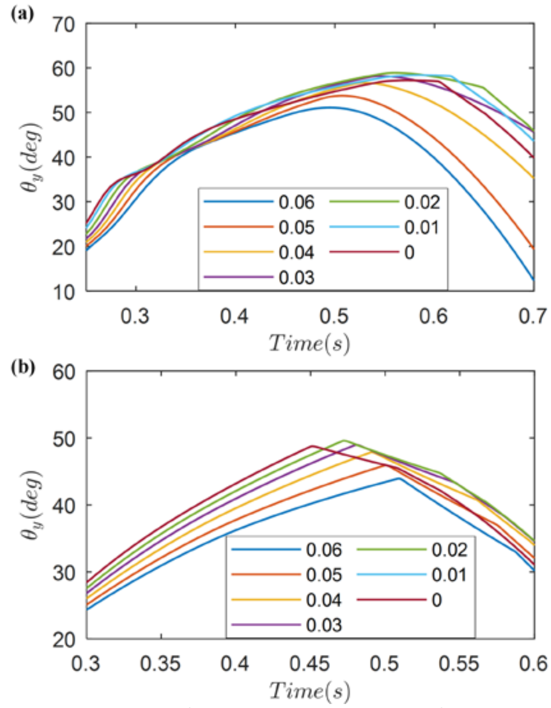

Figure 5. The pitch angle of the model under variations of (a) T_{middle} and (b) T_{fore}.

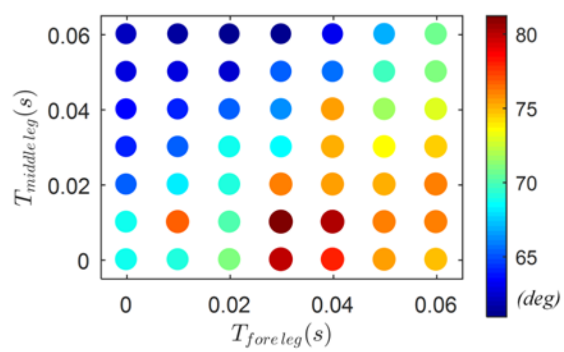

Figure 6. The maximum θ_y of the model with different T_{middle} and T_{fore}.

2) Initial Angle of Torsional Springs on the Legs

The initial angle of torsional springs on the legs affected the normal force from the ground and the contact time between the legs and the ground, which contributed to the θ_y and CoM_z as mentioned in 1). Fig. 7(b) shows the relationship of CoM_z and θ_y with different initial angles of the torsional springs. The trend of the data matched the above prediction.

3) With Actuation of Fore and Middle Legs

When performing a standing long leap, we swung the arms to increase the forward inertia using the remaining four legs. We utilized a step function to trigger the knee angle for simplicity, and the only variable was the final knee angle position, as shown in Fig. 7(c). As the final knee angle approached 270 degrees, the $C\dot{o}M_x$ went higher with the rise of CoM_z.

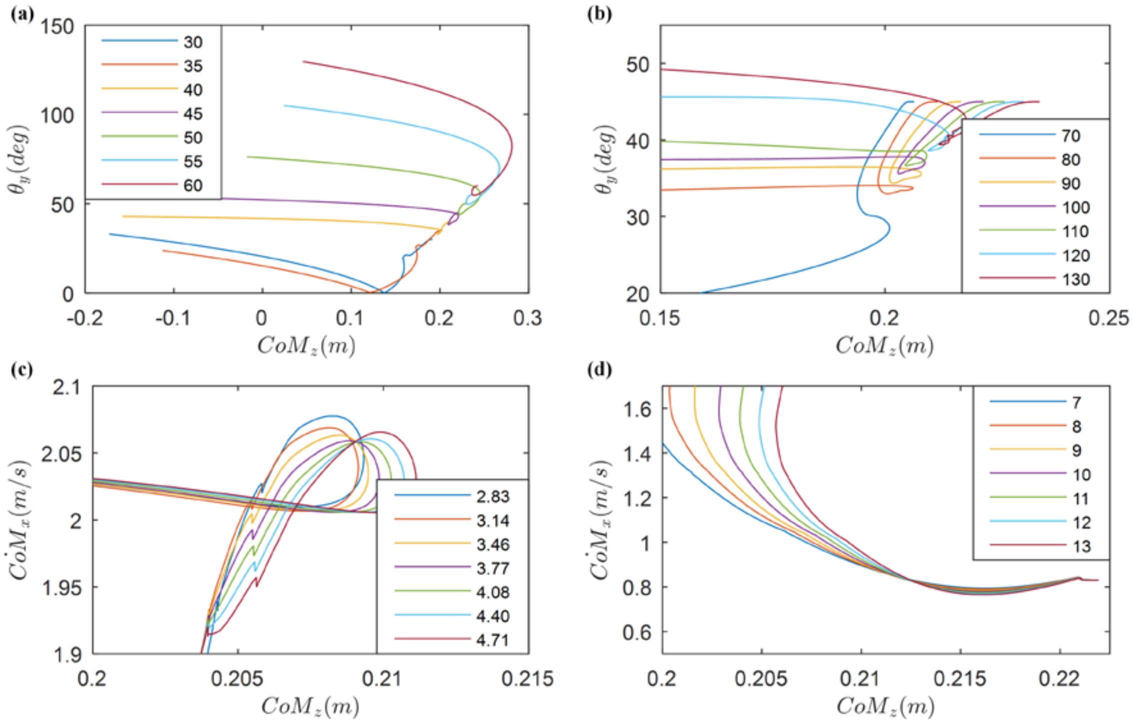

Figure 7. Relations of CoM_z-θ_y and CoM_z - $C\dot{o}M_x$ of the model under parameter variations: (a) initial pitch angle θ_{y,t_0}; (b) initial angle of torsional springs; (c) actuation of fore and middle legs; and (d) the stiffness of the torsional spring.

4) *The Stiffness of the Torsional Springs on the Legs*

The characteristics of the legs may affect the dynamics of the robot, and the selection of different stiffnesses of the torsional spring joint of the legs influenced the energy consumption and the normal force from the ground. Fig. 7(d) shows the plot of CoM_z to $C\dot{o}M_x$ under varied stiffnesses of the torsional springs. The robot had a larger $C\dot{o}M_x$ and higher CoM_z as the stiffness was increased because the springs had a dampening effect and absorbed more energy with less stiffness.

IV. Experiment

The RHex-style robot shown in Fig. 1(a) was used to evaluate the performance of the flip-and-leap gait developed and simulated as previously discussed. A six-axis inertial measurement unit (IMU) was installed in the robot, which allowed the feedback of the pitch angle θ_y.

In this case, the time delay between each pair of legs in the flipping section was selected from the optimization discussed in the Section III. The T_{middle} and T_{fore} were selected to be 40 and 45 ms. The experiments showed that the robot successfully flipped while consuming less energy. Similarly, the leaping pitch angle θ_y was also given by the successful simulation data, which in this case was 130 deg. The final stages of the flipping gait were the main factors that determined whether the flip-and-leap gait was successful. Therefore, the parameters for controlling the flipping gait were tuned precisely to ensure that the flip-and-leap gait would not fail. Fig. 8(a) is a sequence of snapshots taken during the flipping experiment, and Fig. 8(b) is the corresponding simulation in Simulink. Most of the characteristics of the flipping gait in the experiment and the simulation were similar. Due to the energy loss of the slipping condition between the feet and the ground, the maximum height of flipping in the experiment was slightly lower than in the simulation.

The RHex robot needed to process the IMU data in order to determine the timing of leaping. A trivial approach was to directly multiply the $\ddot{CoM}_z$ by the $\cos\theta_y$. When the robot was horizontal, $\ddot{CoM}_z$ should equal the gravity acceleration constant. In our case, the pitch angle of 130 degrees at the beginning of the leaping gait was required, so the leaping gait should be triggered when $\ddot{CoM}_z = -6.3057$ (m/s^2). The IMU data of the flipping gait are shown in Fig. 10, where the unit of $\ddot{CoM}$ was the gravity acceleration constant. The outcome showed that the IMU data were followed by a lot of signal noise.

Further filtering techniques for a more precise triggering point led to latency problem. Therefore, we chose to integrate $\dot{\theta}_y$ for a more accurate estimation of θ_y, and the robot triggered the leaping gait with precise timing. Fig. 9(a) shows the sequence of snapshots during the flip-and-leap experiment, and Fig.9 (b) shows the sequence of the leaping simulation. When the elastic potential energy of the fore pair of legs reached a maximum, the legs underwent a tremendous deformation, which caused the distortion of the R-SLIP model. Therefore, the robot in the simulation could not leap as high as in the experiment.

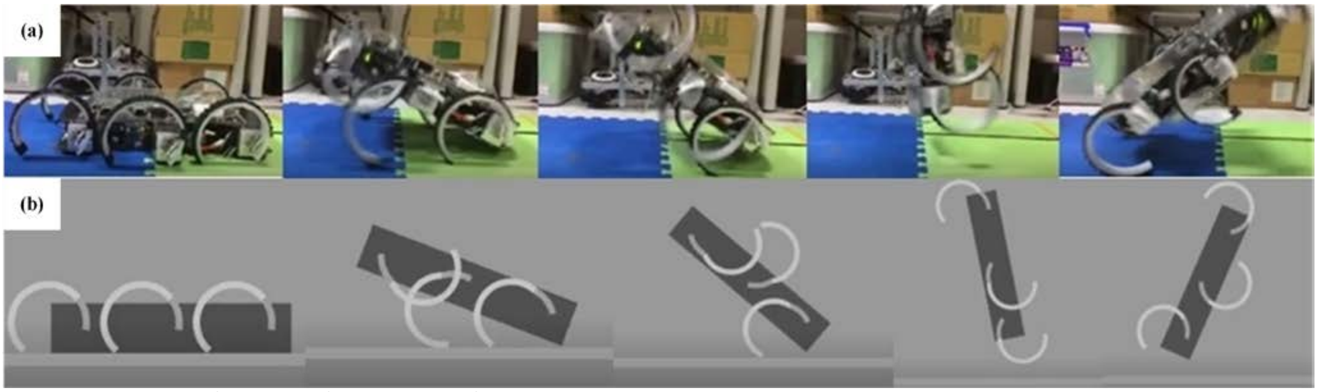

Figure 8. (a) The sequence of snapshots of the robot in the flipping experiment, and (b) the corresponding simulation in Simulink.

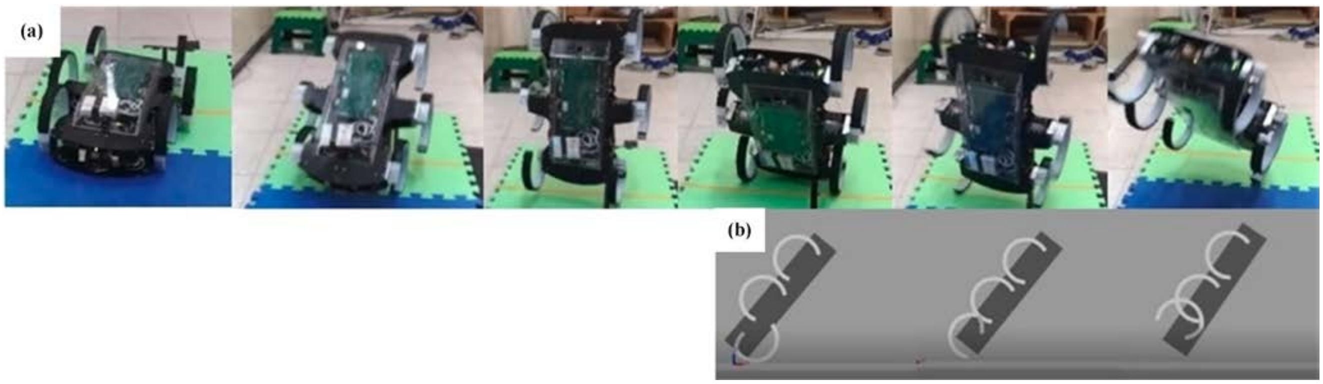

Figure 9. (a) The sequence of snapshots of the robot in the flip-and-leap experiment, and (b) the corresponding simulation in Simulink.

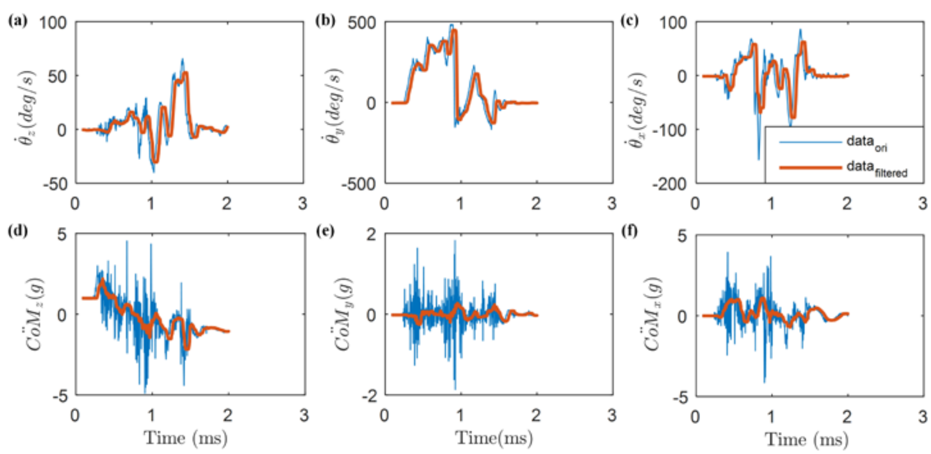

Figure 10. The IMU data of the robot in flipping. The blue and red curves represent raw data and filtered data, respectively.

V. Conclusion

In this paper, we introduced applications based on the flipping gait. Also, we reported on the methodology to optimize the parameters to trigger the flipping and leaping gaits using the R-SLIP model on Simulink, and further realized the gaits on RHex.

To minimize the distortion of the R-SLIP model, we placed the torsional spring position at 50 degrees with respect to the motor shaft and the center of the leg. The parameters, including T_{middle}, T_{fore}, θ_{y,t_0}, angle of torsional spring, actuations of middle legs and rear legs, and stiffness of the torsional springs, were tuned and compared in the simulation. Using the optimization process mentioned in Section III, our robot successfully accomplished the flip-and-leap motion.

Note that although the optimized θ_{y,t_0} was about 40 to 45 degrees, the result was based on the need of highest leaping height. In fact, the robot could adjust the parameters of the leaping gait according to the shape of the stairs to adapt to the terrain and thus increase the efficiency.

A further process of introducing better sensory feedback would allow the robot to know the distance from the target step and allow it to trigger the flip-and-leap gait automatically, providing more versatile usage in the future.

Multimedia

A video of the flipping and leaping with RHex is available at https://youtu.be/1DFbDnFpfCs.

References

[1] Y. Fukuoka, H. Kimura, and A. H. Cohen, "Adaptive dynamic walking of a quadruped robot on irregular terrain based on biological concepts," (in English), *The International Journal of Robotics Research,* Article; Proceedings Paper vol. 22, no. 3-4, pp. 187-202, Mar-Apr 2003, doi: 10.1177/0278364903022003004.
[2] H. Kimura, Y. Fukuoka, and A. H. Cohen, "Adaptive dynamic walking of a quadruped robot on natural ground based on biological concepts," *The International Journal of Robotics Research,* vol. 26, no. 5, pp. 475-490, May 2007. [Online]. Available: <Go to ISI>://000246338400003.
[3] D. J. Hyun, S. Seok, J. Lee, and S. Kim, "High speed trot-running: Implementation of a hierarchical controller using proprioceptive impedance control on the MIT Cheetah," *The International Journal of Robotics Research,* vol. 33, no. 11, pp. 1417-1445, 2014, doi: 10.1177/0278364914532150.
[4] H. W. Park, P. M. Wensing, and S. Kim, "High-speed bounding with the MIT Cheetah 2: Control design and experiments," *The International Journal of Robotics Research,* Article vol. 36, no. 2, pp. 167-192, Feb 2017, doi: 10.1177/0278364917694244.
[5] A. De and D. E. Koditschek, "Vertical hopper compositions for preflexive and feedback-stabilized quadrupedal bounding, pacing, pronking, and trotting," *The International Journal of Robotics Research,* vol. 37, no. 7, pp. 743-778, 2018, doi: 10.1177/0278364918779874.
[6] J. G. Cham, S. A. Bailey, J. E. Clark, R. J. Full, and M. R. Cutkosky, "Fast and robust: Hexapedal robots via shape deposition manufacturing," *International Journal of Robotics Research,* vol. 21, no. 10-11, pp. 869-882, Oct-Nov 2002. [Online]. Available: <Go to ISI>://000181344700005.
[7] J. G. Cham, J. K. Karpick, and M. R. Cutkosky, "Stride period adaptation of a biomimetic running hexapod," *International Journal of Robotics Research,* vol. 23, no. 2, pp. 141-153, Feb 2004. [Online]. Available: <Go to ISI>://000188890700005.
[8] S. Kim, J. E. Clark, and M. R. Cutkosky, "iSprawl: Design and tuning for high-speed autonomous open-loop running," *International Journal of Robotics Research,* vol. 25, no. 9, pp. 903-912, Sep 2006. [Online]. Available: <Go to ISI>://000240939900007.
[9] U. Saranli, M. Buehler, and D. E. Koditschek, "RHex: A simple and highly mobile hexapod robot," *The International Journal of Robotics Research,* vol. 20, no. 7, pp. 616-631, 2001.
[10] U. Saranli, A. A. Rizzi, and D. E. Koditschek, "Model-Based Dynamic Self-Righting Maneuvers for a Hexapedal Robot," *International Journal of Robotics Research,* vol. 23, no. 9, pp. 903-918, 2004, doi: 10.1177/0278364904045594.
[11] G. Dudek *et al.*, "AQUA: an amphibious autonomous robot," *Computer,* vol. 40, no. 1, pp. 46-53, 2007, doi: 10.1109/MC.2007.6.
[12] K. J. Huang, C. K. Huang, and P. C. Lin, "A Simple Running Model with Rolling Contact and Its Role as a Template for Dynamic Locomotion on a Hexapod Robot," *Bioinspiration & Biomimetics,* vol. 9, p. 046004 (20pp), 2014.
[13] E. Z. Moore and M. Buehler, "Stable Stair Climbing in a Simple Hexapod Robot," presented at the International Conference on Climbing and Walking Robots (CLAWAR), 2001.
[14] E. Z. Moore, D. Campbell, F. Grimminger, and M. Buehler, "Reliable Stair Climbing in the Simple Hexapod RHex," in *IEEE International Conference on Robotics and Automation (ICRA)*, 2002, pp. 2222-2227.
[15] D. Campbell and M. Buehler, "Stair Descent in the Simple Hexapod RHex," in *IEEE International Conference on Robotics and Automation (ICRA)*, 2003, pp. 1380-1385.
[16] D. Campbell and M. Buehler, "Preliminary bounding experiments in a dynamic hexapod," *Experimental Robotics VIII,* pp. 612-621, 2003.
[17] D. McMordle and M. Buehler, "Towards pronking with a hexapod robot," Mcgill Research Centre for Intelligemt Machines Montreal (QUEBEC), 2001.
[18] Y. C. Chou, K. J. Huang, W. S. Yu, and P. C. Lin, "Model-Based Development of Leaping in a Hexapod Robot," *IEEE Transactions on Robotics,* vol. 31, no. 1, pp. 40-54, 2015, doi: 10.1109/TRO.2014.2376141.
[19] C. K. Huang, C. L. Chen, C. J. Hu, and P. C. Lin, "Model-based bounding on a quadruped robot," in *IEEE International Conference on Robotics and Automation (ICRA),* 16-21 May 2016 2016, pp. 3576-3581, doi: 10.1109/ICRA.2016.7487540.
[20] R. M. Alexander, *Elastic mechanisms in animal movement* Cambridge University Press 1988.
[21] T. A. McMahon and G. C. Cheng, "The mechanics of running: How does stiffness couple with speed?," *Journal of Biomechanics,* vol. 23, pp. 65-78, 1990, doi: http://dx.doi.org/10.1016/0021-9290(90)90042-2.
[22] M. M. Ankaralı and U. Saranlı, "Control of underactuated planar pronking through an embedded spring-mass Hopper template," *Autonomous Robots,* vol. 30, no. 2, pp. 217-231, 2011, doi: 10.1007/s10514-010-9216-x.
[23] J. Y. Jun and J. E. Clark, "Effect of rolling on running performance," in *IEEE International Conference on Robotics and Automation (ICRA),* 2011, pp. 2009-2014, doi: 10.1109/ICRA.2011.5980433.
[24] C. J. Hu, T. K. H. Wang, C. K., and P. C. Lin, "A torque-actuated dissipative spring loaded inverted pendulum model with rolling contact and its application to hexapod running," *Bioinspiration and Biomimetics,* vol. 14, 2019, Art no. 026005.

Shou-Li Hsu received the double degree of B.S. in mechanical engineering and electrical engineering from National Taiwan University (NTU), Taipei, Taiwan, in 2019. His primary research area pertained to bio-inspired robots, digital integrated circuits, and monolithic mmWave integrated circuits.

Kuan-Wei Liu received the B.S. degree in mechanical engineering from National Taiwan University (NTU), Taipei, Taiwan, in 2019. He is currently studying at Texas A&M University M.S. degree in mechanical engineering at Texas, USA. His current interests include robotic perceptions and motion planning.

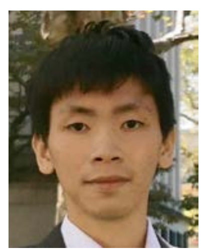

Chia-Ho Hsiung received the bachelor's degree in mechanical engineering from National Taiwan University (NTU), Taipei, Taiwan, in 2019. Currently, He is pursuing his master's degree in mechanical engineering with concentration in robotics and control at Columbia University in the City of New York. He is interested in motion planning and robot learning.

Hsuan-Yu Chen received the B.S. degree in mechanical engineering in 2018 from National Taiwan University (NTU), Taipei, Taiwan, where she is working toward the M.S. degree in mechanical engineering. Her current research interests include mechanism design, robot dynamics and control, and bio-inspired robotics.

Ting-Hao Wang received the B.S. and M.S. degrees in mechanical engineering from National Taiwan University (NTU), Taipei, Taiwan, R.O.C., in 2016 and 2018, respectively. His research interests include mechanism design, dynamics and control, and motion planning.

Pei-Chun Lin received the B.S. and M.S. degrees in mechanical engineering from National Taiwan University (NTU), Taipei, Taiwan, R.O.C., in 1996 and 1998, respectively, and the M.S. degree in electrical engineering and computer science and the Ph.D. degree in mechanical engineering from University of Michigan, Ann Arbor, MI, USA, in 2005.

He was a Postdoctoral Research Fellow in the Department of Materials Science and Engineering, University of Pennsylvania, Philadelphia, PA, USA, from 2005 to 2007. Currently, he is a Professor in the Department of Mechanical Engineering, NTU. His research interests include bio-inspired robotics, mechanical design, sensor design/fusion, control, dynamic locomotion, and compliant composites.